Development of New Beam Configurations for OMEGA to Achieve Highly Uniform Indirect Drive Implosions with Cubic Symmetry

Edward Wu
Pittsford Sutherland High School
Pittsford, NY
Advisor: Dr. R. Stephen Craxton

Laboratory for Laser Energetics
University of Rochester
Rochester, NY
November 2023

Abstract

In light of the recent demonstration of breakeven on the National Ignition Facility (NIF) using indirect drive, interest in future indirect drive facilities has increased. A promising approach is the spherical hohlraum with six laser entrance holes (LEHs), which has cubic symmetry and potentially better uniformity than the cylindrical hohlraum (two LEHs) used on the NIF. While the 60-beam OMEGA laser is primarily a direct drive fusion facility, configurations using a 48-beam subset are proposed that would offer the unique capability of performing highly uniform experiments with a six-LEH hohlraum. Several configurations are possible because beams can be directed into more than one LEH. Using the 3-D code *LORE*, simulations yielded irradiation nonuniformities on the capsule as low as 0.13% (rms) at a high albedo. In addition, the hohlraum radius was varied to investigate the tradeoff between obtaining good uniformity and achieving a high radiation temperature. Beam pointing adjustments were implemented to ensure no beam leakage in designs with small hohlraum radius, demonstrating practicality. Future laser systems based on the OMEGA geometry and designed for direct drive could use these configurations to provide a versatile indirect drive capability.

Keywords: inertial confinement fusion, indirect drive, octahedral hohlraums, OMEGA

Table of Contents

I Introduction

In the 1930s, scientists discovered that nuclear fusion—the combining of two smaller atoms to generate immense amounts of energy—was possible, and was the process that sustained the sun. Later, after the invention of the laser, researchers proposed inertial confinement fusion (ICF), a method in which fuel is heated with a laser so suddenly that the plasma would not have time to escape before it was burned in the fusion reaction.[1] It would be trapped by its own inertia. Today inertial confinement fusion is one of the most promising methods on the path to harnessing nuclear fusion energy. The four-stage process typically involves combining the two isotopes of hydrogen, deuterium (^{2}H) and tritium (^{3}H), as fuel (Fig. 1). This is achieved by containing a small amount of fuel in a shell made of plastic or glass on the scale of a few millimeters and hitting this capsule with high-power lasers. As the shell heats to high temperatures, the outside of the shell ablates outwards while the inside compresses inwards, squeezing the deuterium and tritium (DT) fuel. The compression eventually heats the fuel to such high temperatures while the deuterium and tritium nuclei are pressed close enough that the strong nuclear force is able to overcome the electrostatic force between the positively charged nuclei. The DT is able to fuse into a helium nucleus and release large amounts of energy in the form of energetic neutrons during the sustained nuclear fusion reaction.

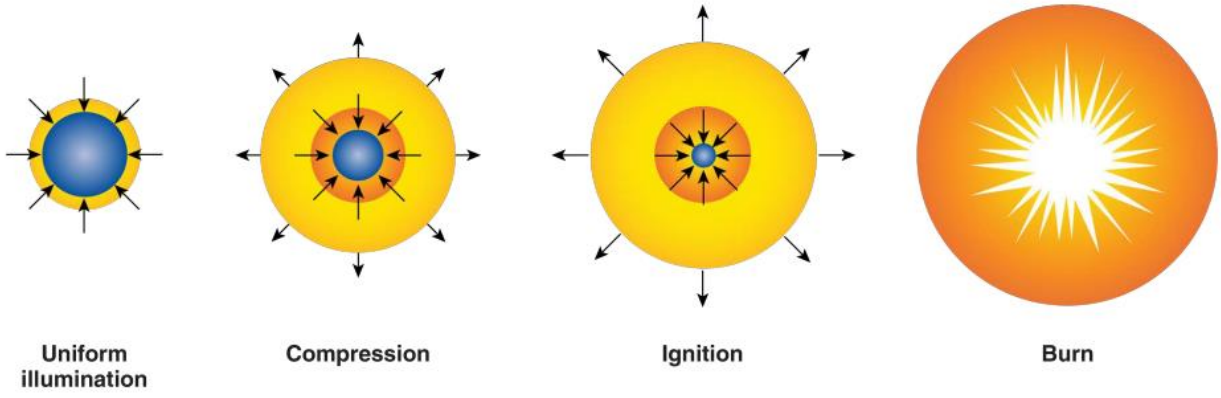

Figure 1. *Four Stages of Inertial Confinement Fusion (ICF). Uniform illumination consists of hitting a capsule (blue) evenly with high-energy lasers. Compression begins as the plastic casing of the capsule starts expanding, resulting in an ablation force inward, squeezing the deuterium and tritium fuel. Ignition occurs when alpha particles deposit energy in the fuel, bringing more fuel to fusion temperatures. Finally, burn is the stage when enough fuel fuses that output energy exceeds input laser energy.*

The two main criteria for achieving ignition from ICF are high uniformity (nonuniformity less than ~1%) and high temperature (50-100 million Kelvin at target center). There are two main approaches to attain these criteria: direct drive[1,2] (Fig. 1) and indirect drive[3] (Fig. 2). In direct drive, laser beams are pointed to hit the capsule and directly irradiate it. While achieving high energy transfer from laser to capsule, this approach suffers from lower levels of uniformity that sometimes compromise the fusion reaction.[2] In addition, direct drive is highly sensitive to slight errors or laser imperfections. Indirect drive (or x-ray drive) is a method in which the capsule is placed inside a case made of high-Z material (typically gold). This gold case is called a hohlraum. There are two types of hohlraums: cylindrical and spherical (as shown in Fig. 2). Instead of directly hitting the capsule, the laser beams enter through laser entrance holes (LEHs) and hit the inner wall of the hohlraum, thereby depositing energy onto the hohlraum. The hohlraum wall then emits x rays, which irradiate the capsule and heat other parts of the inner wall. Due to this more even illumination, indirect drive can have higher uniformity and is less susceptible to imperfections in the laser beams. However, energy transfer is not as efficient as direct drive. Only around 10 to

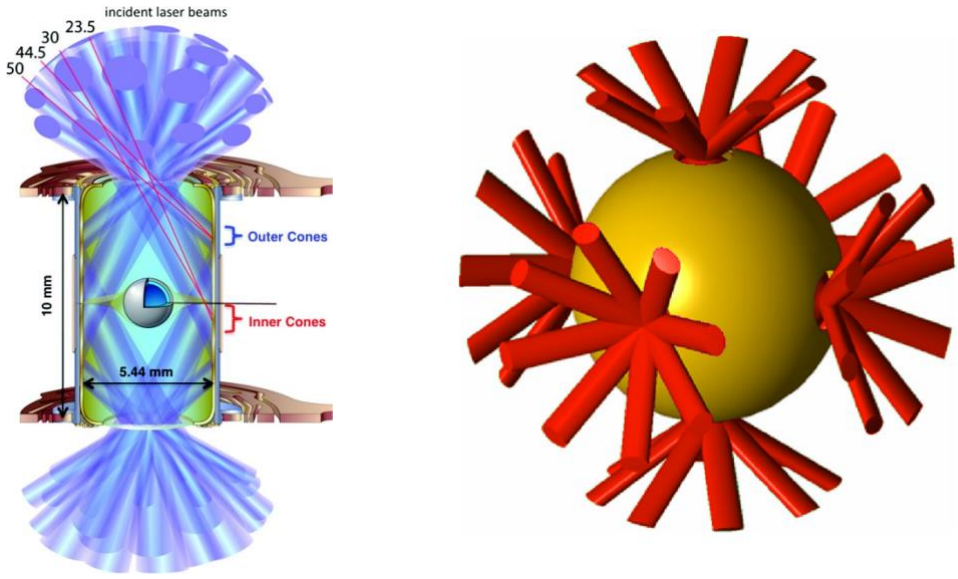

(a) (b)

Figure 2. *Indirect drive. Depicted is the process in which laser beams hit a hohlraum surrounding the capsule, producing x rays which in turn illuminate the capsule more evenly than direct drive. (a) The two-LEH cylindrical hohlraum was shot on the NIF to achieve breakeven. Figure from Ref. 4. (b) The spherical octahedral hohlraum with six LEHs is a proposed hohlraum for improved future indirect drive ignition. Figure from Ref. 5.*

20% of the laser energy is absorbed by the capsule in indirect drive as opposed to 80 to 90% in direct drive. This study focuses on indirect drive.

The two most powerful ICF lasers in the United States are OMEGA at the Laboratory for Laser Energetics, designed for direct drive, and the National Ignition Facility (NIF) at the Lawrence Livermore National Laboratory, designed for indirect drive. Because these laser systems have different intended methods of achieving ICF, the OMEGA system and NIF have significant differences in their beam layout. OMEGA has 60 laser beams distributed in a highly symmetrical configuration[6] based a truncated icosahedron ("soccer ball") with 12 pentagonal and 20 hexagonal faces (Fig. 3). The NIF has four rings of beam ports located at angles of 23.5°, 30.0°, 44.5°, and 50.0° from the vertical in the upper hemisphere (Fig. 2(a)). A symmetrical arrangement is present in the lower hemisphere. In total, the NIF contains 48 quads, which are groups of four beams.

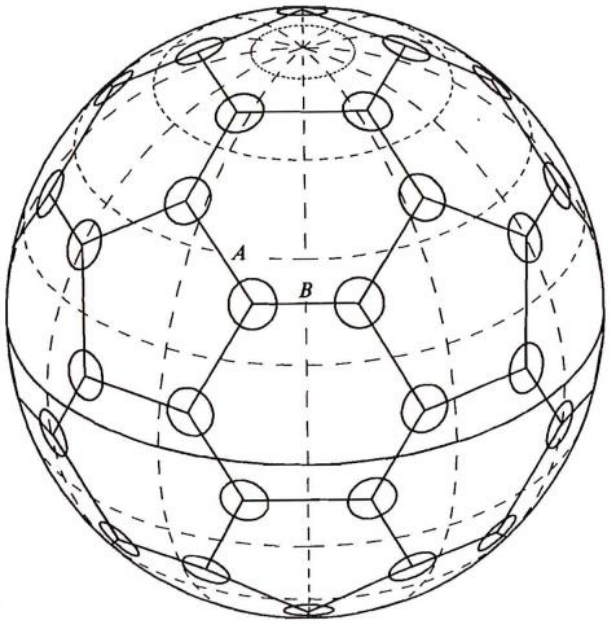

Figure 3. *Omega Geometry. 60 beams are evenly distributed on a sphere in a stretched-soccer-ball geometry. A/B=1.2. Figure from Ref. 6.*

In December 2022, the NIF achieved a historic milestone with a shot that demonstrated breakeven for the very first time, outputting 3.15 MJ of energy from a 2.05 MJ input of laser light for an energy gain of about 1.5.[7-9] A cylindrical hohlraum with two polar LEHs, shown in Fig. 2(a), was used. One criticism of this hohlraum design is that the fuel capsule will implode nonuniformly due to a lack of drive on the equatorial region of the capsule at later times in the

reaction. The NIF overcame this issue by "tuning," in which the specific pointings of the beams can be adjusted and the powers of the inner (23.5°, 30°) and outer (44.5°, 50°) beams can be varied during the pulse to achieve a greater uniformity. However, tuning is challenging and takes considerable time.

Thus, spherical hohlraums have been proposed and developed as a more promising way to achieve higher uniformity and consistency. The tetrahedral hohlraum (Fig. 4(a)) is a geometry that has four LEHs located corresponding the vertices of a tetrahedron. Around 2000, tetrahedral hohlraums were shot on OMEGA and shown to achieve high levels of uniformity.[10]

Recently, octahedral hohlraums (Fig. 4(b)) have been proposed as an even more uniform alternative to the cylindrical and tetrahedral hohlraums.[11-13] The octahedral hohlraum has six LEHs corresponding to the vertices of an octahedron (or centers of cube faces). However, neither the

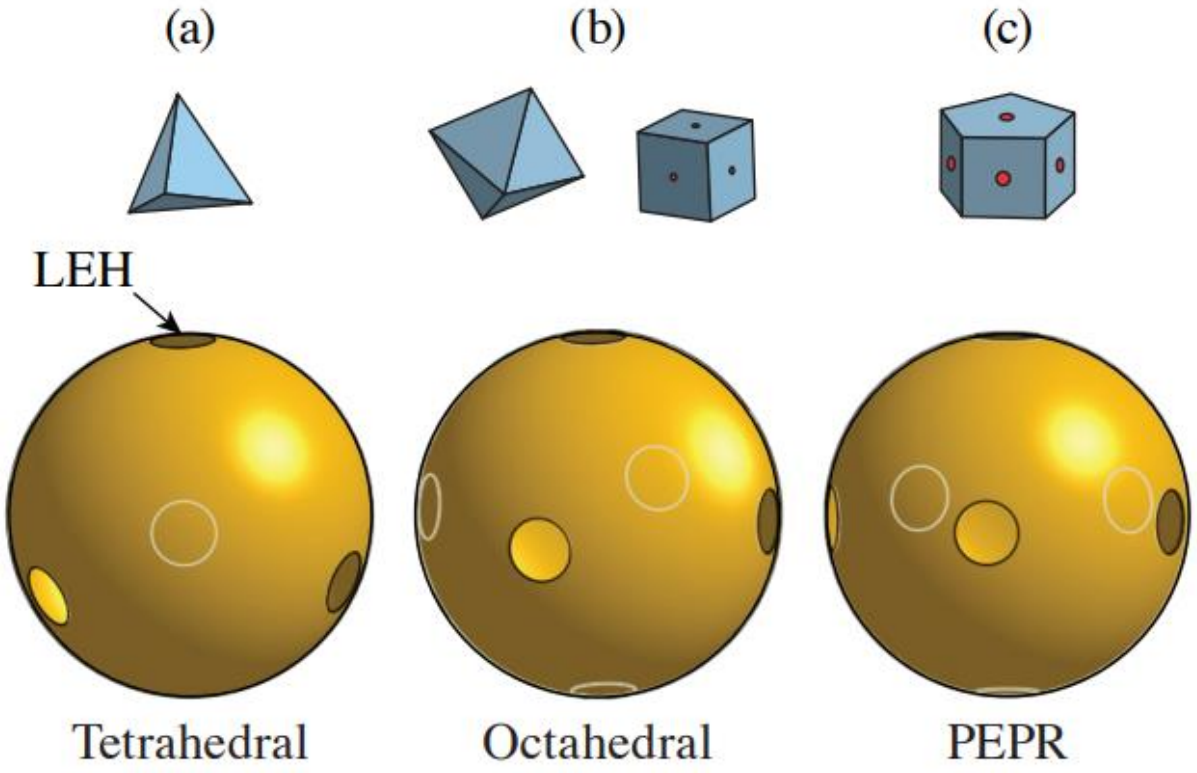

Figure 4. *Spherical Hohlraum Designs. (a) A tetrahedral hohlraum with 4 LEHs that has been shot on OMEGA. (b) An octahedral hohlraum with 6 LEHs (4 equatorial and 2 polar) that has been proposed as a very promising design for increased uniformity. (c) A pentagonal prism (PEPR) hohlraum with 7 LEHs (5 equatorial and 2 polar) that has been proposed for OMEGA. Figure from Ref. 14.*

NIF nor the conventional 60-beam OMEGA match the cubic symmetry of the octahedral hohlraum and as a result cannot drive it.

In an effort to support spherical indirect drive on OMEGA, the Pentagonal Prism (PEPR) hohlraum (Fig. 4(c)) was proposed.[14] PEPR has seven LEHs with five LEHs on the equator corresponding to the centers of the lateral faces of a pentagonal prism and two polar LEHs corresponding to the centers of the base faces of said pentagonal prism. PEPR allows all 60 beams of OMEGA to be used in an indirect drive experiment. To evaluate its performance, simulations were done using *LORE*,[14] a three-dimensional (3-D) code that evaluates uniformity on a capsule for indirect drive on a spherical hohlraum. *LORE* predicts that PEPR achieves nonuniformities on the capsule of 1.1% (rms) early in the laser pulse to 0.6% later in the pulse. In general, around 1% nonuniformity is believed to be needed in order to achieve ignition.[2] However, PEPR has limited symmetry as the polar holes get half as many laser beams as the equatorial holes do.

The SGIV Laser[15] is a proposed Chinese ICF facility that is planned to be a NIF-sized system intended to drive spherical hohlraums. Recently, on the existing cylindrically configured 48-beam SGIII Laser, a 32-beam laser repointing scheme was developed to allow an octahedral hohlraum to be shot, optimized for highest radiation temperature and irradiation symmetry. This scheme was experimentally carried out with success in showing proof-of-concept. Additional work has been carried out on optimizing LEH size for ignition-scale octahedral hohlraums, specifically on SGIII.[16,17]

The present work develops configurations for a 48-beam subset of OMEGA that would allow for octahedral hohlraums to be driven with cubic symmetry on OMEGA. The code *LORE* predicts nonuniformities well under 1% for all configurations tested. The tradeoffs between hohlraum-to-capsule diameter ratio, uniformity, and background radiation temperature have been explored and several beam pointings were calculated to test the limits of this design, showing that it can confidently be shot on OMEGA and is applicable to future OMEGA-like direct drive laser systems.

II OMEGA Indirect Drive Design

The 60 beams on OMEGA can be partitioned into two subsets: a 24-beam subset and a 36-beam subset[18] as shown in Fig. 5, which is a projection of the full 360° surface of the sphere. The horizontal and vertical dotted lines represent lines of latitude and longitude, while the solid lines represent cube edges. In addition, the light blue shaded area indicates a pair of pentagons from the OMEGA geometry, one such pair per face. The 24-beam subset is represented by the beams shaded in blue ("A" group) and the 36-beam subset is represented by the beams shaded in purple and beams left white ("B" and "C" groups). As both beam subsets have cubic symmetry, the configuration allows for a two-step zooming technique,[19,20] which involves sending two consecutive temporal pulses, one from each subset, with different spot sizes, to improve laser coupling efficiency and increase energy gain. In zooming, the smaller laser spots come later to follow the imploding target. This can be applied to future 60-beam OMEGA-like systems.

We propose that a 48-beam subset of the OMEGA beams can be used to perform indirect drive using an octahedral hohlraum with cubic symmetry. As shown in Fig. 5, 48 shaded beams can be activated to drive a six-LEH hohlraum. This configuration would allow 8 beams to be driven

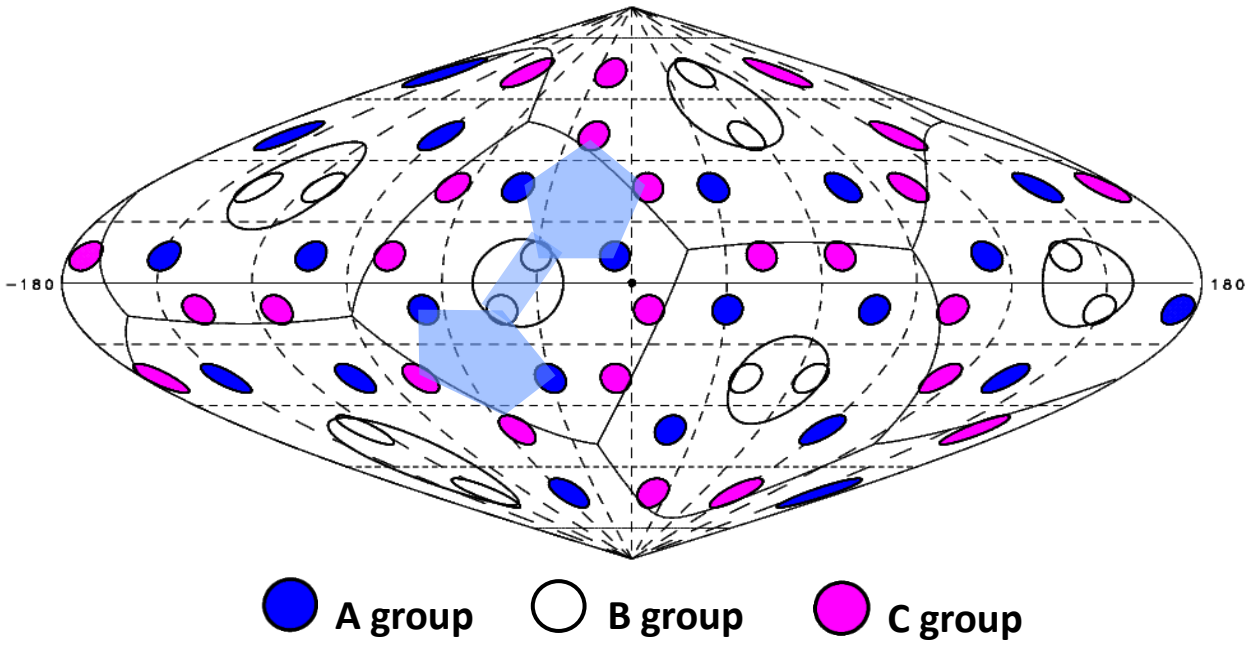

Figure 5. *Colored beam map of OMEGA. The 48-beam configuration is proposed for driving an octahedral hohlraum with cubic symmetry. Cube edges and LEH holes are drawn and beams are split into three groupings. A group and C group beams are colored to show that they can be used for indirect drive. B group beams are empty to show that they cannot be used for indirect drive.*

into each LEH, preserving symmetry on all sides of the hohlraum. One group of beams denoted "B" cannot be used for indirect drive at all due to their angle with respect to the LEHs. An attempt to use the "B" group would cause the beams to hit the capsule.

Angle of incidence θ_i refers to the angle in which a beam enters an LEH, specifically the angle between the beam direction and the normal to the LEH. We first propose the "default" configuration of the "A" beams entering their closest LEH at $\theta_i = 31°$ and the "C" beams entering the same LEH at $\theta_i = 42°$ staying consistent with the pentagonal geometry of OMEGA, shaded in light blue in Fig. 5.

The 8 beams enter their assigned LEH the exact same way for every other LEH on the octahedral hohlraum. However, from Fig. 6, the "A" group can also enter two further LEHs at angles of 67° and 70° and the "C" group can enter a neighboring LEH at 50°. Thus, there are 6 distinct combinations of matching beams to LEHs. Each of these six configurations is investigated and evaluated with respect to uniformity, feasibility, and even distribution. These six configurations allow for significant flexibility in selecting a desired pairing of "A" and "C" beams. Furthermore, because there is 5-fold symmetry about the vertical axis, there are additionally five

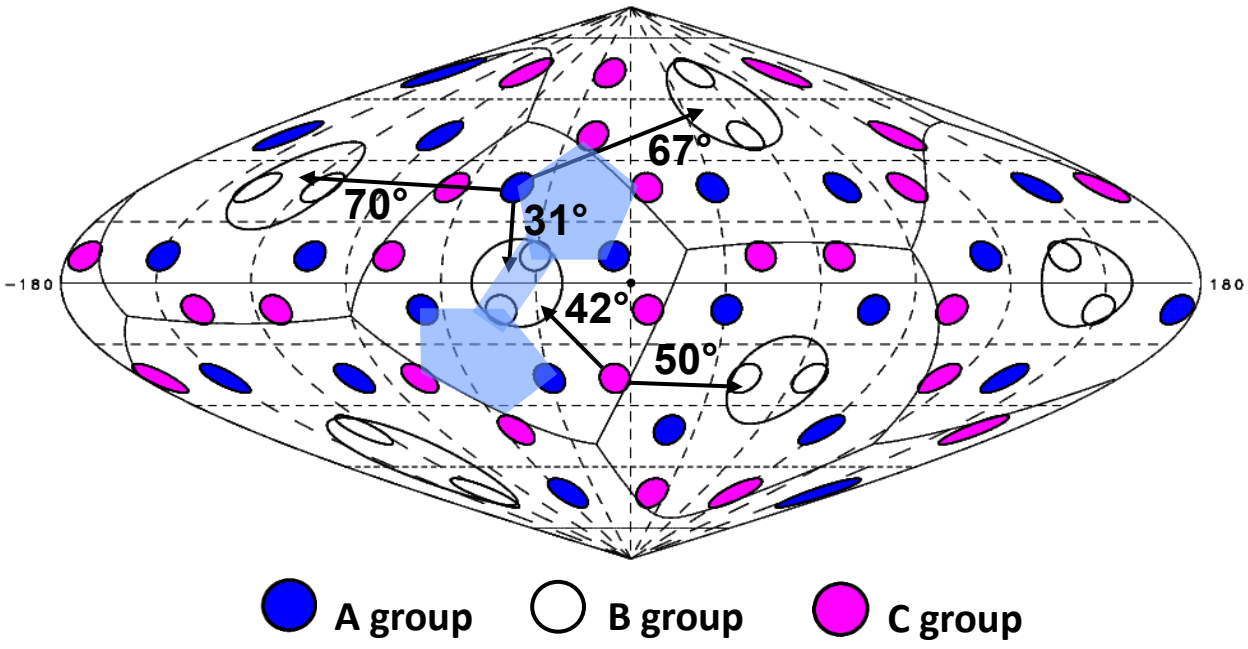

***Figure 6**. Beam-LEH configurations. The "A" Group of beams have three LEH options with angles of incidence of 31°, 67°, and 70°. The "C" Group of beams have two LEH options with angles of incidence of 50° and 42°. Therefore, there are six distinct and plausible configurations with this 48-beam subset.*

distinct rotations that exactly mimic each other in behavior. This can allow for flexibility in selecting the best rotation to allow for the choice of instrument diagnostics needed for a desired experiment.

III Illustrative Simulation

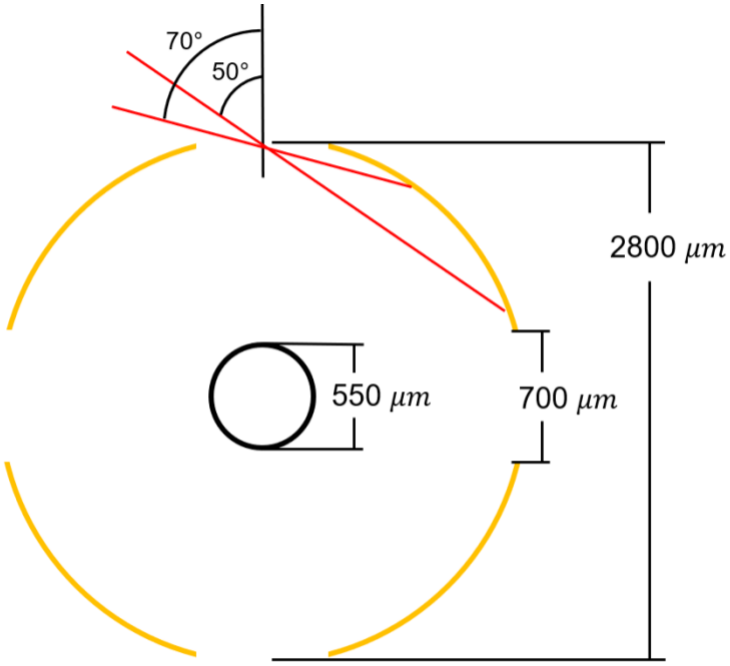

Figure 7. *Hohlraum dimensions and ray paths for OMEGA. Diameter of capsule is 550 μm, diameters of LEHs are 700 μm, and diameter of hohlraum is 2800 μm. Note that the diameter of the hohlraum can be shrunk to achieve higher temperatures. Rays with angles of incidence of 70° and 50° are also shown.*

Figure 7 shows the octahedral hohlraum dimensions for OMEGA. Simulations were done using *LORE*. It begins by tracing rays in 3-D from each laser beam, from the center of the LEH the beam passes through. The radius of the beam is typically half of the radius of the LEH. The beam cross section is converted into a 2-D grid of one million individual rays, each parallel to the beam direction (Fig. 8).

LORE then finds where the rays make contact with the hohlraum wall. At this intersection a fraction of the energy is deposited, given by the equation,

$$A(\theta) = 1 - \exp\left(-b * \cos^{r}(\theta)\right) \quad (1)$$

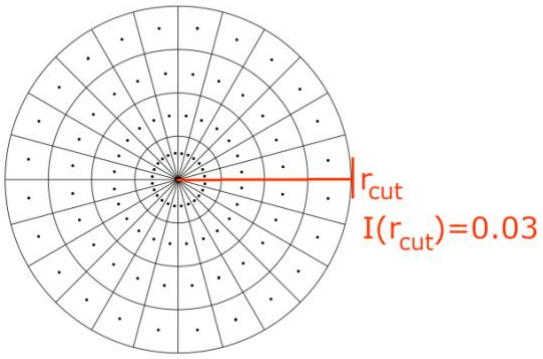

Figure 8. *2-D grid of beam cross section. Each cell contains one point, which represents the starting location of a ray.* r_{cut} *represents the maximum radius that rays are defined.*

where θ is the angle of incidence on the hohlraum wall (e.g. θ = 31°, 50°, 70°). The values of b and r are taken to be 3 and 1, respectively.[21] Hohlraums typically absorb a high level of incident laser energy on the first intersection. If a bounce is needed, *LORE* reflects the ray and determines the second intersection.

The deposited laser energy plot (Fig. 9(a)) has $A(\theta) = 1$, meaning only one intersection will be calculated by *LORE*. The ideal deposited laser energy plot has minimal overlap and an even spread of laser spots on the hohlraum wall. The "A" and "C" beam spots are labeled in Fig. 9. $A(\theta) = 1$ is just to illustrate the first beam spots. Figure 9(b) also shows the second and third bounces according to Eqn. (1).

LORE next calculates the background, or equilibrium, radiation temperature T_r by balancing power entering the radiation field with power lost due to the LEHs and absorption by the hohlraum wall and capsule using the equation,

$$P_{las}\eta_{\mathrm{L}} = \sigma T_r^4 (NA_h + B_w A_w + B_c A_c) \qquad (2)$$

where P_{las} is the power of all the beams added together, η_L represents the efficiency of the conversion of laser energy to x-ray energy, which is typically taken to be in the range of 0.65 to 0.8, and σ is the Stefan-Boltzmann constant. N represents the number of LEHs and A_h, A_w, A_c represent the areas of the LEHs, hohlraum wall, and capsule, respectively. B_w is the fraction of the background radiation energy absorbed by the hohlraum wall, which is also equal to $1 - \alpha_w$, where the albedo α_w increases as the hohlraum wall heats up. The albedo is a time-dependent variable.

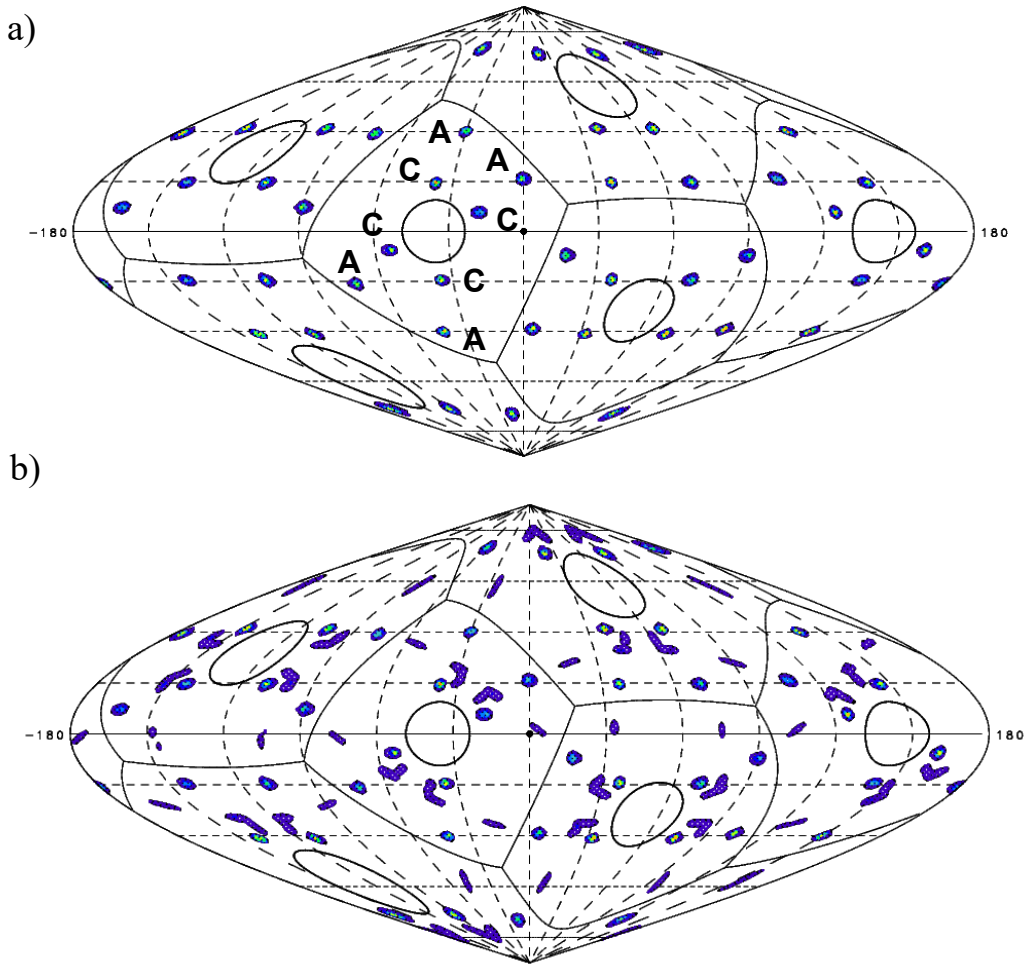

Figure 9. *Deposited laser energy on hohlraum wall as calculated by LORE for the 67°, 50° configuration. (a) Bounce parameter turned off, which is why there are only first bounces shown. LEHs are indicated with outlines. "C" beams land close to the LEHs and "A" beams are more distant. (b) First, second, and third bounces shown according to Eqn. (1).*

B_c is the fraction of background radiation energy absorbed by the capsule, which is usually set to around 0.9.

After calculating the background radiation temperature, *LORE* calculates the effective radiation temperature, T_e, at every point on the hohlraum wall with the equation,

$$\sigma T_e^4 = \alpha_w \sigma T_r^4 + \eta_L I_L \tag{3}$$

where σT_e^4 is the radiation flux emitted by the wall, $\alpha_w \sigma T_r^4$ is the background radiation flux that is reflected by the hohlraum wall (power/unit area), and $\eta_L I_L$ is the fraction of absorbed laser power per unit area converted to radiation.

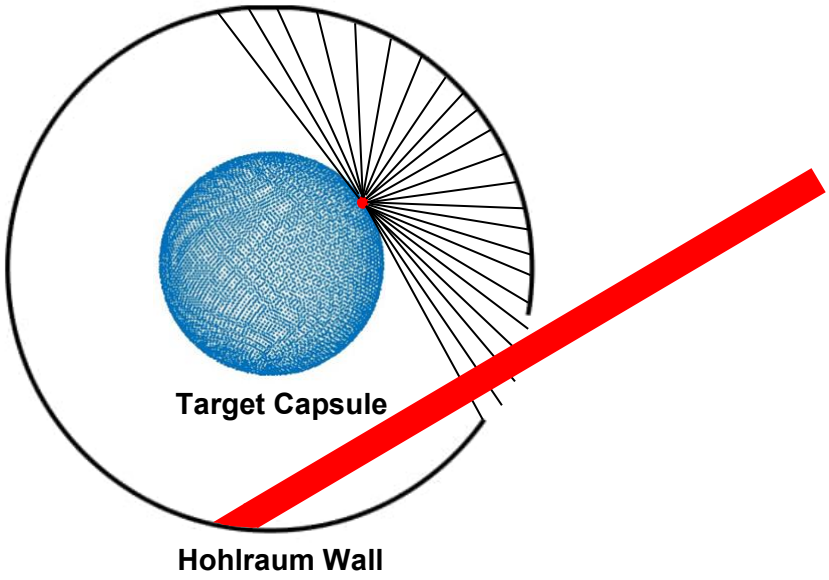

Figure 10. *Calculating uniformity on a capsule. The code LORE starts by depositing laser energy on the hohlraum wall. Then the code scans over many points on the capsule and for each point scans over the direction coming from the hohlraum wall for spectral brightness to calculate the radiation intensity at that point on the capsule.*

After calculating the effective radiation temperature, *LORE* scans over multiple points on the capsule and integrates the spectral brightness ($\sigma T_e^4/\pi$) over all angles (Fig. 10). Radiation intensity can be calculated through the equation,

$$I = \int_0^{\frac{\pi}{2}} \int_0^{2\pi} B(\theta, \phi) \cos(\theta) \sin(\theta)\, d\phi d\theta \tag{4}$$

where θ and ϕ are the direction altitude and direction azimuth, respectively. The $\cos(\theta)$ accounts for the angle between the surface element of the capsule and the incoming ray and the $\sin(\theta)$ accounts for the solid angle. $B(\theta, \phi)$ is spectral brightness, $\sigma T_e^4/\pi$, the power emitted per unit area per unit solid angle from the hohlraum wall. As shown in Fig. 11 for the 67°, 50° configuration, *LORE* then produces uniformity contour plots of the radiation flux experienced by the capsule and calculates the nonuniformity (rms). This integration process involves scanning 60,000 points on the capsule and for each point, looking over 100,000 directions.

Because *LORE* has no time dependent parameter, we represent this through wall albedo. As the ICF reaction proceeds, the wall albedo α_w increases over time. Thus, we can treat wall

albedo as analogous to time. Figure 11 is a uniformity plot with α_w = 0.9, which represents the latter end of the indirect drive ICF process, giving a nonuniformity = 0.125%.

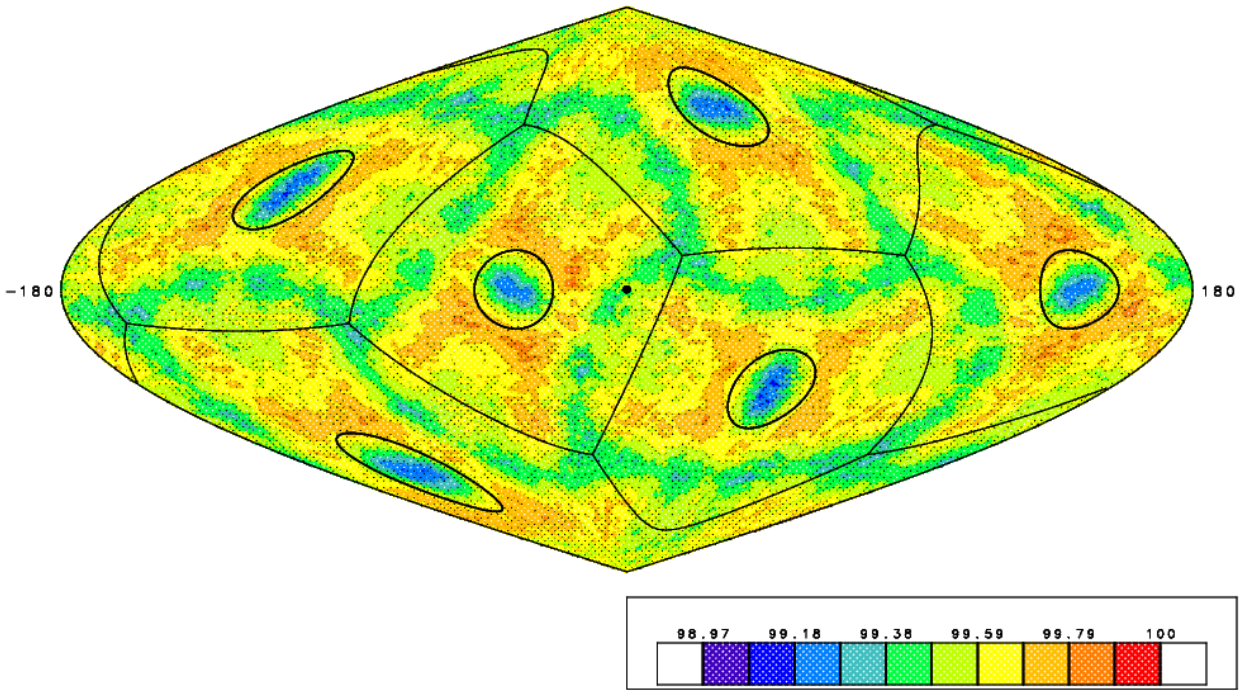

Figure 11. *Capsule uniformity contour plot as percent of maximum for the 67°, 50° case shown in Fig. 9 taken at an albedo α_w of 0.9. Nonuniformity (rms) = 0.125%.*

IV Results

IV.1 Analysis of the 6 beam-LEH configurations

Figure 12 shows the nonuniformities of the six distinct beam-LEH configurations. These calculations were done at an early time (albedo = 0.1) and beams were pointed through the center of the LEHs. Note that the default configuration (left) does not perform the best, rather the 67°, 50° configuration yields the lowest nonuniformity of 0.48%. However, all configurations are highly practical being well under the recommended 1% nonuniformity and have low variability with a range of only 0.14%.

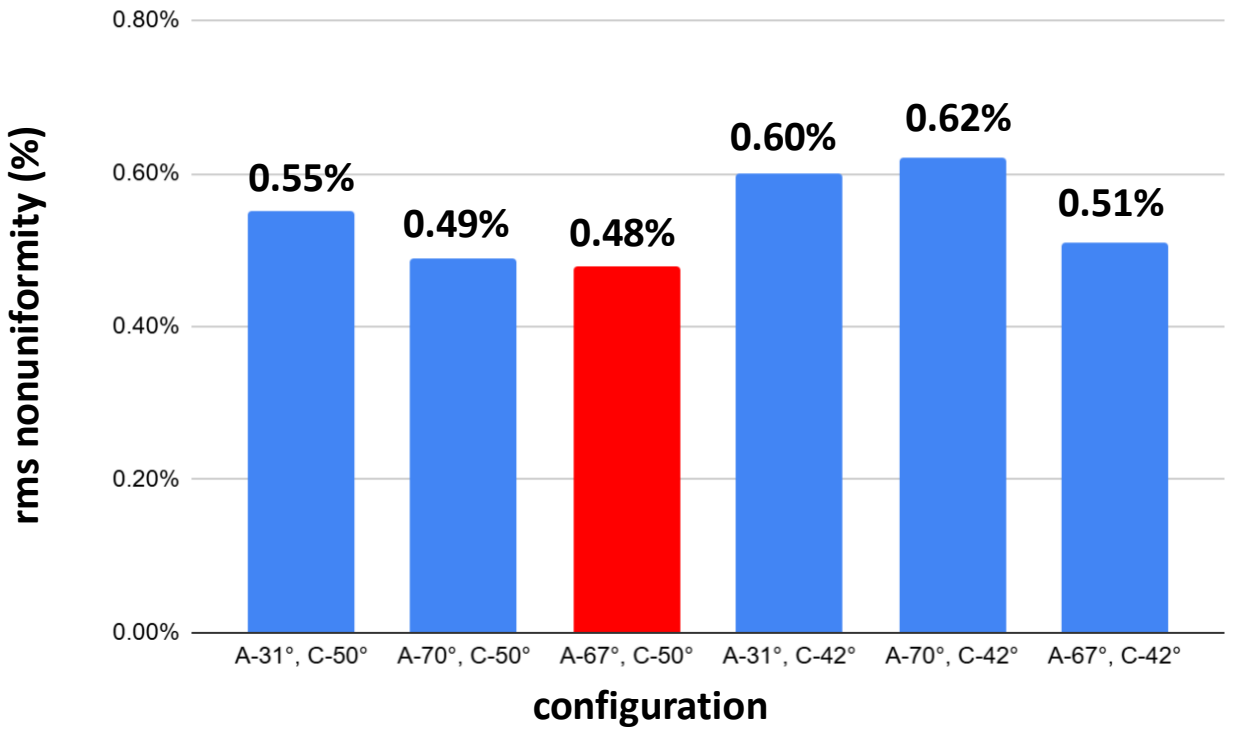

Figure 12. *Nonuniformities of the six distinct beam-LEH configurations for a wall albedo of 0.1. Highlighted in red is the "best" configuration with the lowest nonuniformity.*

The ideal angle of incidence θ_i ranges from 55° to 60°.[11] Beams entering at an angle of incidence less than 55° risk leaving through another LEH, undesirably hitting the capsule, or crossing with other beams. Beams entering at an angle of incidence greater than 60° have the risk of coming too close to an LEH and ablating the gold wall.[11] This can cause plasma formation close to the LEH, which may block the paths of incoming beams at later times. However, for practical implementation, this angle range must be extended. The tetrahedral hohlraum, which was shot on OMEGA in 2000, had θ_i ranging from 23.2° to 58.8°. When selecting one of the six beam-LEH configurations of the 48-beam design, angle of incidence can be taken to account. The 67°, 50° configuration may be preferred as it has the closest angles to the ideal 55° to 60° range while also having the lowest nonuniformity of 0.48%.

IV.2 Nonuniformity over time

Analysis of capsule nonuniformity over time is important to see how the implosion will progress and whether any undesirable squeezing of the capsule will occur where one area of the

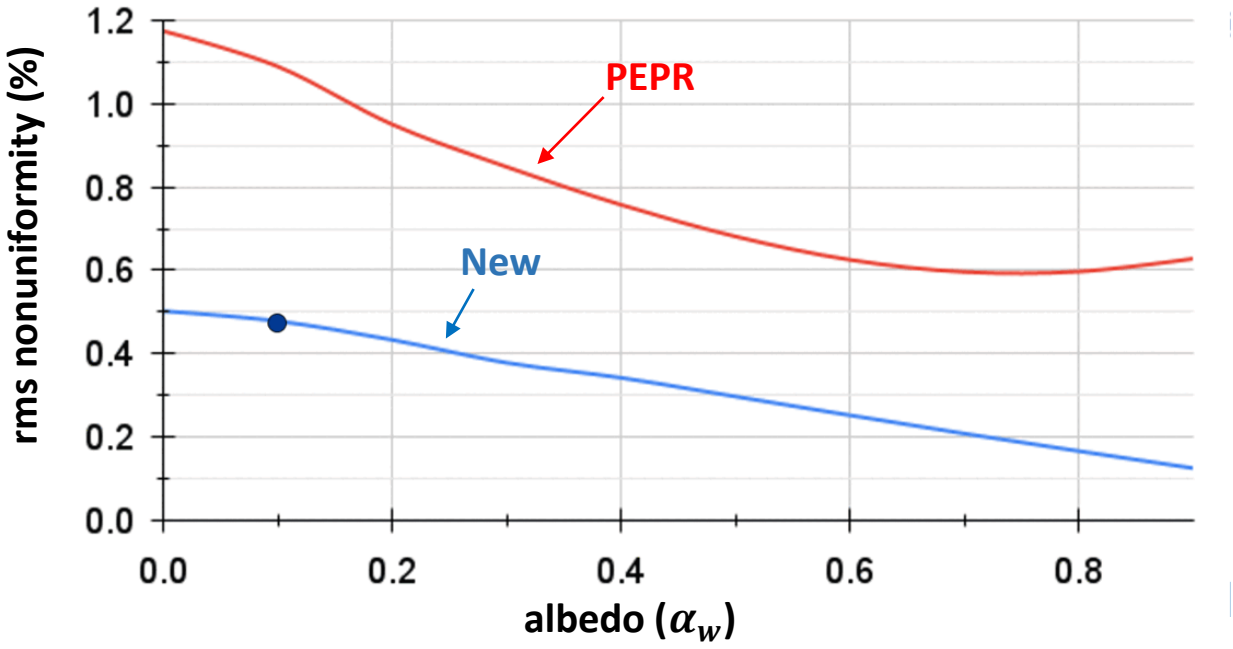

Figure 13. *Nonuniformity as a function of wall albedo. The blue line shows the new best 48-beam configuration (67°, 50°) and the red line shows the optimized PEPR design. The blue dot shows the 48-beam configuration at an albedo of 0.1 as it was compared to the five other configurations.*

shell will compress quicker leading to an uneven compression. Figure 13 shows a comparison of capsule nonuniformity between the "best" 67°, 50° configuration and the 7-LEH pentagonal prism hohlraum, PEPR. Even with PEPR's optimized beam pointing adjustments, the 48-beam configuration has lower nonuniformity by a factor of 2 at every albedo, without any repointings. Beam repointings are adjustments that can be made to change the best focus points of beams with respect to the center of the LEH (default pointing). For the 48-beam design, all beams currently go through the LEH centers. At albedo = 0.7, the capsule nonuniformity of the PEPR hohlraum begins to increase; however, the 48-beam configuration consistently decreases in nonuniformity at a steady and approximately linear rate.

IV.3 Background radiation temperature tradeoff

The background radiation temperature T_r is another important metric for all hohlraum designs. On OMEGA, P_{las} is taken to be 18 TW. For the current OMEGA dimensions of 275 μm

for the capsule radius, 350 μm for the LEH radius, and 1400 μm for the hohlraum radius, the radiation temperature is calculated to be 212 eV.

To achieve a higher radiation temperature, the hohlraum radius can be shrunk; however, this results in a lower capsule uniformity. The beam and LEH sizes are kept the same. Therefore, as the hohlraum is sized-down, beams may risk hitting the capsule directly or begin to leak out of LEHs, significantly diminishing both the radiation temperature and uniformity of an implosion (Fig. 14(a)). Beam repointings shifting the best focus points away from the center of the LEH were done on the 31°, 50° design to ensure no leakage occurred, even on the smallest hohlraum radii

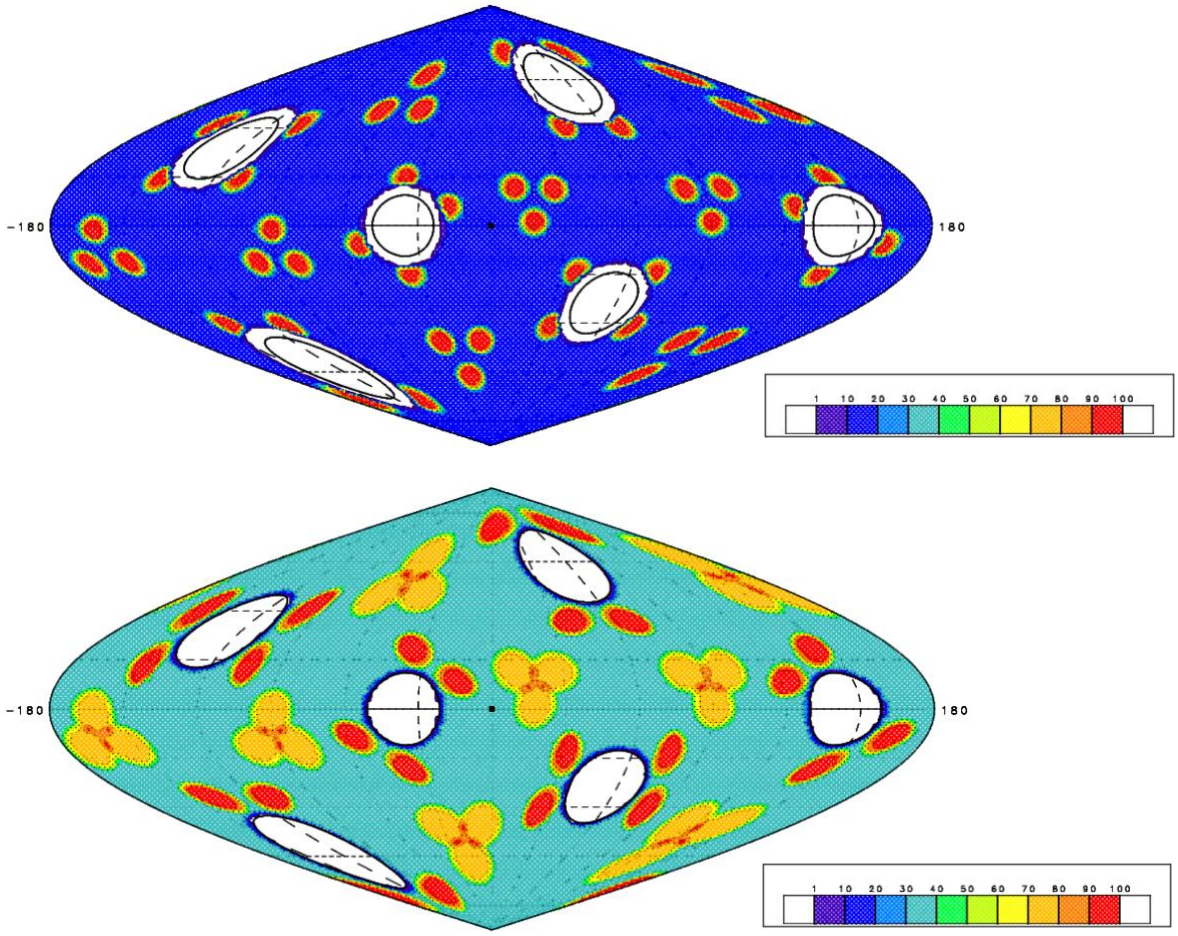

Figure 14. *Effective radiation temperature plots as percent of maximum for the 31°, 50° configuration with OMEGA dimensions and hohlraum radius = 960 μm. (a) Pointing through LEH centers, beam leakage can be seen near the LEHs. This decreases the uniformity and radiation temperature of the implosion. (b) Beams repointed, leakage is alleviated. The difference in colors is due to differing P_{las} values and having a single bounce included in the effective radiation temperature calculation (a) versus having multiple bounces included in the calculation (b).*

(Fig. 14(b)). These repointings also demonstrate the practicality of the 48-beam designs for actual experiments using these configurations on OMEGA.

In regards to the tradeoff between radiation temperature and capsule uniformity based on the hohlraum radius to capsule radius ratio, the new repointings were used to ensure no unwanted beam leakage. Figure 15 shows the capsule nonuniformity while the hohlraum radius is varied (the

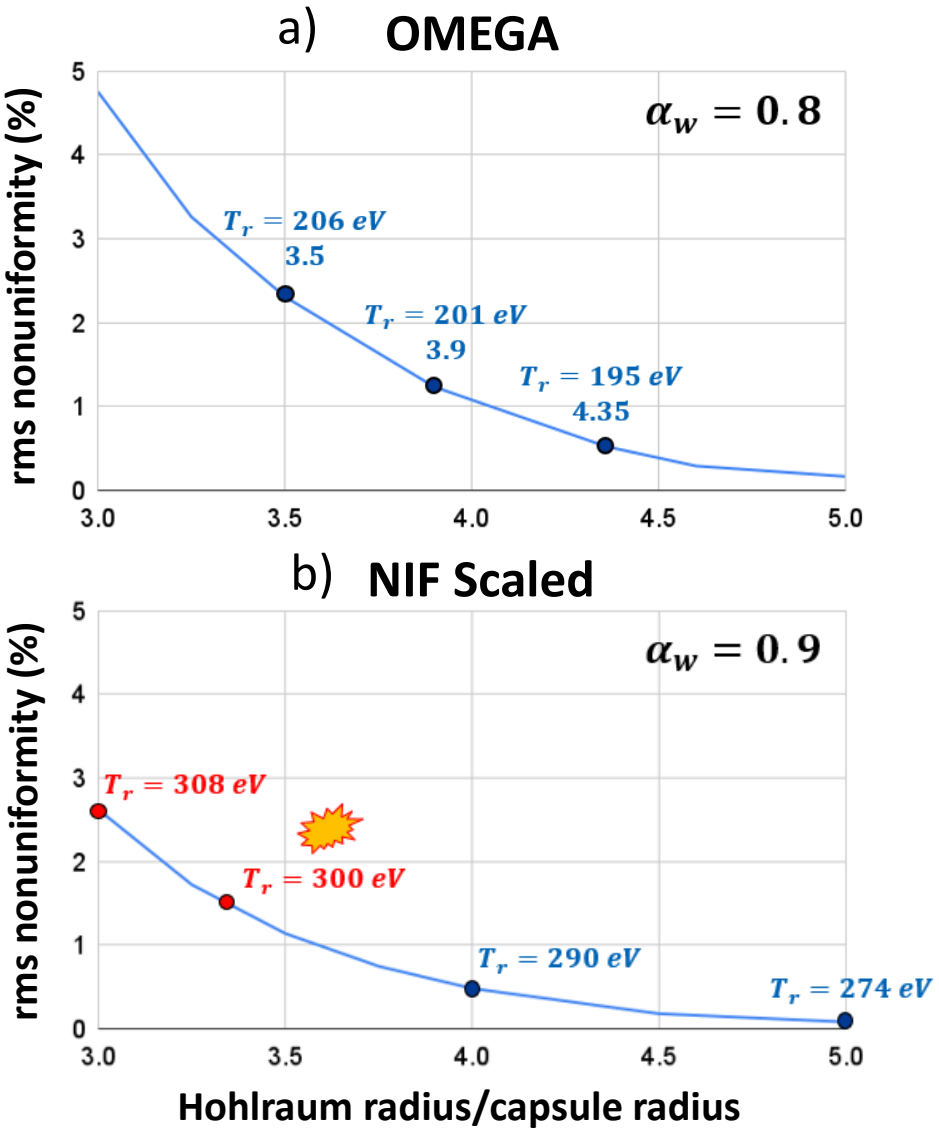

Figure 15. *Tradeoff of rms nonuniformity with respect to hohlraum-to-capsule radius. (a) Nonuniformity is plotted as a function of the ratio of hohlraum radius to capsule radius on OMEGA. The radiation temperatures are shown. (b) Nonuniformity is plotted as a function of the ratio of hohlraum radius to capsule radius on a NIF-scale system with 500 TW power (still OMEGA geometry). The radiation temperatures are shown. Red values show temperatures ≥ 300 eV generally acknowledged as needed to achieve ignition.*

capsule and LEH radii are kept the same). The same repointings were used for each simulation. As seen in Fig. 15(a), as hohlraum-to-capsule ratio is decreased, capsule nonuniformity is increased substantially, but the radiation temperature is increased. As an example of this tradeoff, a hohlraum-to-capsule ratio of 4.35 gives a nonuniformity of 0.52% and a T_r of 195 eV. At a hohlraum-to-capsule ratio of 3.5, a nonuniformity of 2.31% is reached, with an increased T_r of 206 eV. With the beam repointings, no leakage occurred at any of these points.

While this new 48-beam subset is designed to drive octahedral hohlraums on the OMEGA facility, it is instructive to scale it to an ignition-size system to show that the temperature threshold for ignition of around 300 eV can be met. Figure 15(b) shows the 48-beam subset configuration scaled to a NIF-size power. The capsule diameter is increased from 550 μm to 2.2 mm, the LEH diameter is increased from 700 μm to 2 mm, and P_{las} is increased from 18 TW to 500 TW, as on the NIF. Wall albedo α_w was increased to 0.9 as bigger hohlraums produce a higher albedo because a thicker layer of hot gold is created, which makes it harder for radiation to escape into the wall. The 300 eV threshold is achieved by this configuration with a hohlraum-to-capsule ratio of 3.35 and a nonuniformity of 1.43%. An even lower ratio of 3.0 achieves a T_r of 308 eV and nonuniformity of 2.619%, which is too high to reliably achieve ignition. No leakage occurred in this case.

V Conclusions

Spherical hohlraums are currently of high interest in achieving superior uniformity for ignition from ICF as compared to cylindrical hohlraums as used on the NIF. Specifically, the 6-LEH octahedral hohlraum has been proposed to achieve the lowest levels of nonuniformity. Recognizing the need to test these octahedral hohlraums before large-scale laser systems are built for the hohlraum, this work proposes experiments on the 60-beam OMEGA laser using several configurations of a 48-beam subset.

The 48-beam configurations have been intensively simulated and show very good capsule uniformities, without any beam repointings. For the best “A” beam/”C” beam configuration of 67°, 50°, nonuniformities are calculated to be 0.48% at low albedos to 0.125% at high albedos, which improves over PEPR’s nonuniformity (0.6% at high albedos) nearly five-fold. Importantly, this 48-beam design offers cubic symmetry, which is needed for octahedral hohlraums and mimics

future large-scale laser systems sending 8 beams into each of the 6 LEHs of an octahedral hohlraum.

The 48-beam configurations offer a platform for the performance of a variety of experiments. The platform can be used to show high-quality octahedral hohlraum implosions with zero tuning compared to the campaigns at the NIF, which require extensive tuning. The six distinct configurations allow for flexibility in choosing optimal angles of incidence and the diagnostics needed. Furthermore, the fivefold rotational symmetry of the OMEGA target chamber allows even more flexibility for all experiments. To achieve a higher radiation temperature, the ratio of hohlraum-to-capsule radii can be decreased. This, however, leads to a tradeoff with capsule uniformity. On OMEGA, the radiation temperature can be increased from 195 to 206 eV by shrinking the hohlraum radius as nonuniformity increases from 0.522% to 2.309%. On a NIF-scaled system, the 300 eV threshold is achieved with a nonuniformity of 1.43%.

As research on ICF continues at a rapid pace, the 48-beam configurations provide a useful test bed for 3D modeling on octahedral hohlraums. In addition, the implosions can be generated on OMEGA, offering a platform for the examination of highly uniform indirect drive implosions. Lastly, these 48-beam configurations show a reliable way for future OMEGA-like direct drive systems to also have a uniform and improved method of indirect drive.

Acknowledgements

I would like to thank my advisor, Dr. Stephen Craxton, for giving me valuable suggestions throughout my project and providing feedback on my data analysis and simulations. I would also like to thank William Wang for useful conversations helping me get started with *LORE*. Finally, I am very grateful for the Laser Lab Summer High School Research Program and everyone involved for giving me the opportunity to research nuclear fusion at the Laboratory for Laser Energetics.

References

[1]J. Nuckolls, L. Wood, A. Thiessen, and G. Zimmerman, "Laser compression of matter to super-high densities: Thermonuclear (CTR) applications," Nature **239**, 139 (1972).

[2]R. S. Craxton, K. S. Anderson, T. R. Boehly, V. N. Goncharov, D. R. Harding, J. P. Knauer, R. L. McCrory, P. W. McKenty, D. D. Meyerhofer, J. F. Myatt, A. J. Schmitt, J. D. Sethian, R. W. Short, S. Skupsky, W. Theobald, W. L. Kruer, K. Tanaka, R. Betti, T. J. B. Collins, J. A. Delettrez, S. X. Hu, J. A. Marozas, A. V. Maximov, D. T. Michel, P. B. Radha, S. P. Regan, T. C. Sangster, W. Seka, A. A. Solodov, J. M. Soures, C. Stoeckl, J. D. Zuegel, "Direct-drive inertial confinement fusion: A review," Phys. Plasmas **22**, 110501 (2015).

[3]J. D. Lindl, "Development of the indirect-drive approach to inertial confinement fusion and the target physics basis for ignition and gain," Phys. Plasmas **2**, 3933 (1995).

[4]D. E. Hinkel, M. D. Rosen, E. A. Williams, A. B. Langdon, C. H. Still, D. A. Callahan, J. D. Moody, P. A. Michel, R. P. J. Town, R. A. London, and S. H. Langer, "Stimulated Raman scatter analyses of experiments conducted at the National Ignition Facility," Phys. Plasmas **18**, 056312 (2011).

[5]L. Jing, S. Jiang, L. Kuang, L. Zhang, L. Li, L. Zhang, H. Li, J. Zheng, F. Hu, Y. Huang, T. Huang, and Y. Ding, "Preliminary study on a tetrahedral hohlraum with four half-cylindrical cavities for indirectly driven inertial confinement fusion," Nucl. Fusion **57**, 046020 (2017).

[6]A. Simon (editor), "The OMEGA Upgrade Part II: Preliminary Design and Target System," LLE Review, Quarterly Report, Univ. Roch. **39**, 113 (1989).

[7]D. Clery, "Explosion marks laser fusion breakthrough," Science **378**, 1154 (2022).

[8]J. Tollefson and E. Gibney, "Nuclear-fusion lab achieves 'ignition': What does

it mean?," Nature **612**, 597 (2022).

[9]B. Bishop, see *https://www.llnl.gov/news/national-ignition-facility-achieves-fusion-ignition* for "National Ignition Facility Achieves Fusion Ignition."

[10]J. Wallace, T.J. Murphy, N.D. Delamater, K.A. Klare, J.A. Oertel, G.R. Magelssen, E.L. Lindman, A. Hauer, P.L. Gobby, J.D. Schnittman, R.S. Craxton, W. Seka, R.L. Kremens, D.K.

Bradley, S.M. Pollaine, R.E. Turner, O.L. Landen, D.M. Drake, and J.J. Macfarlane, "Inertial Confinement Fusion with Tetrahedral Hohlraums at OMEGA," Phys. Rev. Lett. **82**, 3807 (1999).

[11]K. Lan, X.-T. He, J. Liu, W. Zheng, and D. Lai, "Octahedral spherical hohlraum and its laser arrangement for inertial fusion," Phys. Plasmas **21**, 052704 (2014).

[12]K. Lan and W. Zheng, "Novel spherical hohlraum with cylindrical laser entrance holes and shields," Phys. Plasmas **21**, 090704 (2014).

[13]K. Lan, J. Liu, D. Lai, W. Zheng, and X.-T. He, "High flux symmetry of the spherical hohlraum with octahedral 6 LEHs at the hohlraum-to-capsule radius ratio of 5.14," Phys. Plasmas **21**, 010704 (2014).

[14]W.Y. Wang and R.S. Craxton, "Pentagonal Prism Spherical Hohlraums for OMEGA," Phys. Plasmas **28**, 062703 (2021).

[15]X.T. Hea, and W.Y. Zhang, "Advances in the national inertial fusion program of China," EPJ Web of Conferences **59**, 01009 (2013).

[16]H. Cao, X. Xie, Y. Chen, Y. Dong, L. Wang, Z. Cao, X. Chen, Q. Wang, W. Zhou, W. Zhang, Z. Li, S. Li, B. Deng, H. Liang, S. Li, J.F. Wu, G. Ren, X. Hang, W.Y. Huo, X. Huang, X. Peng, D. Yang, T. Xu, L. Hou, X. Che, L. Guo, H. Du, X. He, C. Li, P. Yang, Q. Gu, Y. Wang, K. Zheng, Y. Huang, F. Bao, Y. Gao, B. Jiang, H. Zhang, F. Wang, J. Yang, S. Liu, J. Xie, Z. He, K. Du, J. Liu, S. Zou, Y. Ding, Q. Zhu, and K. Lan, "Laser repointing scheme for octahedral spherical hohlraums on the SGIII laser facility," Phys. Plasmas **30**, 042703 (2023).

[17]Y. Chen, Z. Li, H. Cao, K. Pan, S. Li, X. Xie, B. Deng, Q. Wang, Z. Cao, L. Hou, X. Che, P. Yang, Y. Li, X. He, T. Xu, Y. Liu, Y. Li, X. Liu, H. Zhang, W. Zhang, B. Jiang, J. Xie, W. Zhou, X. Huang, W.Y. Huo, G. Ren, K. Li, X. Hang, S. Li, C. Zhai, J. Liu, S. Zou, Y. Ding, and K. Lan, "Determination of laser entrance hole size for ignition-scale octahedral spherical hohlraums," Matter Radiat. Extremes **7**, 065901 (2022).

[18]M. Temporal, A.R. Piriz, B. Canaud, R. Ramis, and R.S. Craxton, "Partition of Omega-like facility into two configurations of 24 and 36 laser beams to improve implosion performance," Scientific Reports **13**, 10010 (2023).

[19]R.H. Lehmberg and J. Goldhar, "Use of Incoherence to Produce Smooth and Controllable Irradiation Profiles with KrF Fusion Lasers," Fusion Technol. **11**, 532 (1987).

[20]B. Canaud and F. Garaude, "Optimization of laser–target coupling efficiency for direct drive laser fusion," Nucl. Fusion **45**, L43 (2005).

[21]J.D. Schnittman and R.S. Craxton, "Three-dimensional modeling of capsule implosions in OMEGA tetrahedral hohlraums," Phys. Plasmas **7**, 2964 (2000).